



## Feasibility of hard X-ray imaging using monolithic active pixel sensors (MAPS)

Xuan Li <sup>a,\*</sup>, Zhehui Wang <sup>a</sup>, Pinghan Chu <sup>a</sup>, Cesar da Silva <sup>a</sup>, Melynda Brooks <sup>a</sup>, Christopher M. O'Shaughnessy <sup>a</sup>, Chris Morris <sup>a</sup>, Ming Liu <sup>a</sup>, Sho Uemura <sup>a</sup>, Marcel Demarteau <sup>b</sup>, Robert Wagner <sup>b</sup>, Junqi Xie <sup>b</sup>, Ren-Yuan Zhu <sup>c</sup>, Liyuan Zhang <sup>c</sup>, Chen Hu <sup>c</sup>

<sup>a</sup> Los Alamos National Laboratory, Physics Division, Los Alamos, NM 87545, USA

<sup>b</sup> Argonne National Laboratory, High Energy Physics Division, Lemont, IL 60439, USA

<sup>c</sup> California Institute of Technology, Physics Division, Pasadena, CA, 91125, USA

### ARTICLE INFO

#### Keywords:

Silicon detector  
Monolithic active pixel sensor  
Hard X-ray imaging

### ABSTRACT

Silicon detectors have been widely used in high energy physics (HEP) experiments. The outstanding properties of silicon detectors include radiation hardness, small material budget, fine spatial resolution, high speed and low cost. Here we report initial results of using a single-bit Monolithic Active Pixel Sensor (MAPS), a leading candidate for the next generation trackers in high luminosity colliders, for hard X-ray imaging. The MAPS responses to X-ray with different energies are obtained and compared with simulation. The observed cluster sizes are larger than that predicted by the Continuous Slowing Down Approximation (CSDA) model, indicating that the charge diffusion process might play an important role in the MAPS response to low energy electrons. This work paves the way towards multiple layer ultrafast silicon sensor applications in synchrotrons and XFEL beamlines.

### Contents

1. Introduction .....	1
2. Experiment setup and results .....	1
3. Summary and outlook .....	5
Acknowledgments .....	5
References .....	5

## 1. Introduction

Two essential hardware elements of high-speed imaging are a bright source of illumination and a fast camera that can match the temporal or pulse-to-pulse structure of the source. With the anticipated introduction of 88 MHz mode of hard X-ray source operation at the Advanced Photon Source (APS), a highly efficient hard X-ray camera becomes a critical component in order to achieve nearly 10 ns imaging frame-time. Considering the fact that dedicated camera technology development can take over a decade from concept to a working prototype and requires substantial investments, we verified the feasibility of applying the high-speed fine silicon pixel sensors that include the Monolithic Active Pixel Sensor (MAPS) technology, being developed for high-luminosity hadron colliders, for high-speed hard X-ray imaging application through an X-ray source and possibly for use at a synchrotron such as the APS (see Fig. 1).

## 2. Experiment setup and results

X-rays interact with silicon through photoelectric absorption, Compton scattering and coherent scattering, and the cross sections are X-ray energy dependent. Early tests of the 28  $\mu\text{m}$  by 28  $\mu\text{m}$  pixel MAPS sensor with 100  $\mu\text{m}$  thickness [1] developed by the ALICE collaboration have demonstrated good sensitivity to soft X-rays ( $E_{\text{photon}} = 5.9$  keV or 6.5 keV) generated by a  $^{55}\text{Fe}$  source [2]. Hard X-rays ( $E_{\text{photon}} > 10$  keV) can penetrate through multiple layers of MAPS sensors. To understand the silicon sensor energy and spatial response to hard X-rays, we started with the X-ray source test using a commercial pixel sensor: Pixelink PL-D725MU which can measure the photon intensity per pixel. Then we tested the ALICE MAPS sensor with the same setup. The Pixelink silicon sensor contains 5  $\mu\text{m} \times 5 \mu\text{m}$  pixels and its thickness is at least a factor of two larger than the ALICE MAPS sensor. For the initial work, our goals are: (a) To obtain proof-of-principle results for hard X-ray imaging

\* Corresponding author.

E-mail address: [xuanli@lanl.gov](mailto:xuanli@lanl.gov) (X. Li).

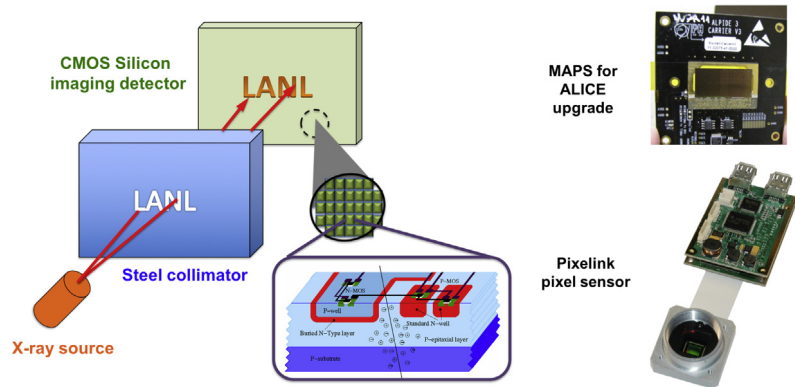


Fig. 1. The proof-of-concept experiment setup using silicon sensors with a “LANL” logo collimator. The silicon sensor options include the ALICE MAPS and the Pixelink pixel sensor, other detector techniques are considered and will be included in future tests.

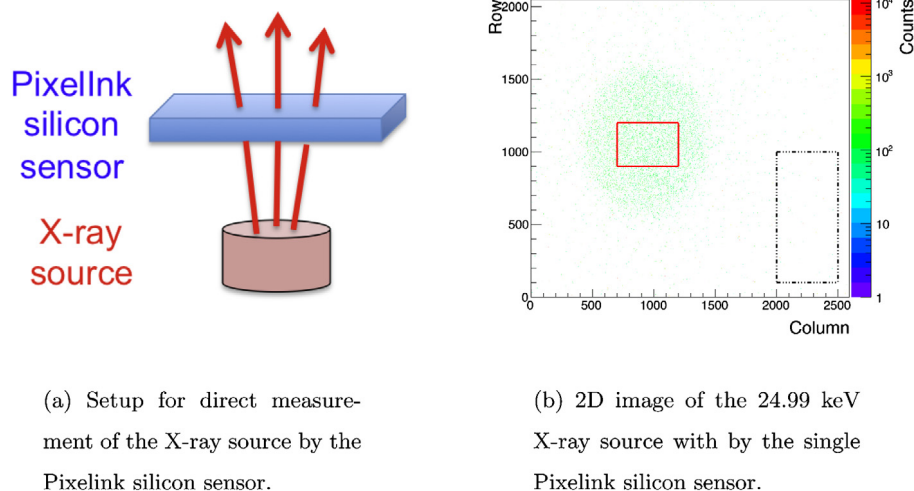


Fig. 2. Direct measurements of the X-ray source using the Pixelink silicon sensor. The setup is shown in (a) and the 2D imaging plot of X-ray source with 24.99 keV energy is shown in (b). A source dominant region (red solid box) and a background contamination region (black dashed box) are selected.

using the Pixelink silicon pixel sensor and the ALICE MAPS sensor; (b) To characterize the silicon pixel sensor spatial and energy performance experimentally and compare them with simulations; (c) To come up with designs that can be tested at the APS.

For the X-ray imaging feasibility test, one Pixelink silicon sensor and an  $^{241}\text{Am}$  X-ray source with a wide range of characterization energy (both  $K\beta$  and  $K\alpha$ ) have been used. This  $^{241}\text{Am}$  X-ray source can vary the emitted X-ray energy from 8.91 keV to 50.65 keV by selecting different targets, which allows us to study the silicon pixel sensor performance in both soft and hard X-ray regions. Fig. 2a shows the setup for direct X-ray measurements with the single layer Pixelink silicon sensor. Fig. 2b shows the 2D imaging plots of the X-ray source with 24.99 keV energy measured by the Pixelink sensor. A threshold bounded cluster finder was applied on the X-ray imaging plots to form clusters from adjacent pixels with measured photon intensity larger than 10% of its maximum value. To better understand the spatial and energy resolution of the Pixelink sensor, a X-ray source dominant region and a background contaminated region are selected as shown in Fig. 2b to study the cluster size and cluster integrated photon intensity (referred to as the cluster energy).

As shown in Fig. 3, the average cluster size for 24.99 keV X-rays measured by the Pixelink silicon sensor is around 3 pixels. This indicates the spatial resolution of the Pixelink silicon sensor with  $5\ \mu\text{m}$  pixels is better than  $5\ \mu\text{m}$ . Scattered photons or electrons have higher probabilities to be measured in the background contaminated region than direct X-ray

photons or electrons. Therefore cluster energy and cluster size measured in the background contaminated region are smaller than those probed in the source dominant region as shown in Fig. 3. Moreover, a clear energy characterization peak has been found in the cluster energy distribution measured in the source dominant region using 24.99 keV X-rays (see top right panel of Fig. 3). The mean value of the characterization peak is defined as the cluster characterization energy. The average cluster size and the average cluster energy have been determined for each energy value provided by the X-ray source. The cluster characterization energy has been measured for each energy except 8.91 keV, where the energy is too low for a clear characterization peak. Fig. 4 summarized the X-ray energy dependent average cluster size, the average cluster energy and the cluster characterization energy for the Pixelink silicon sensor. The linear increase of the cluster characterization energy with the X-ray energy suggests that events within the cluster characterization peak region have X-rays fully absorbed by the Pixelink sensor. For X-ray energy less than 30 keV, the interaction between the X-ray and the silicon sensor is dominated by photoelectric absorption and a trend of increasing cluster size or energy with the X-ray energy is observed. When the energy of X-ray exceeds around 30 keV, Compton scattering starts to dominate. Less energy gets deposited in the silicon sensor and more X-rays penetrate through the detector, which leads to smaller cluster size and cluster energy. To evaluate the dependence of the X-ray detection efficiency on X-ray energy and the sensor thickness, the FLUKA

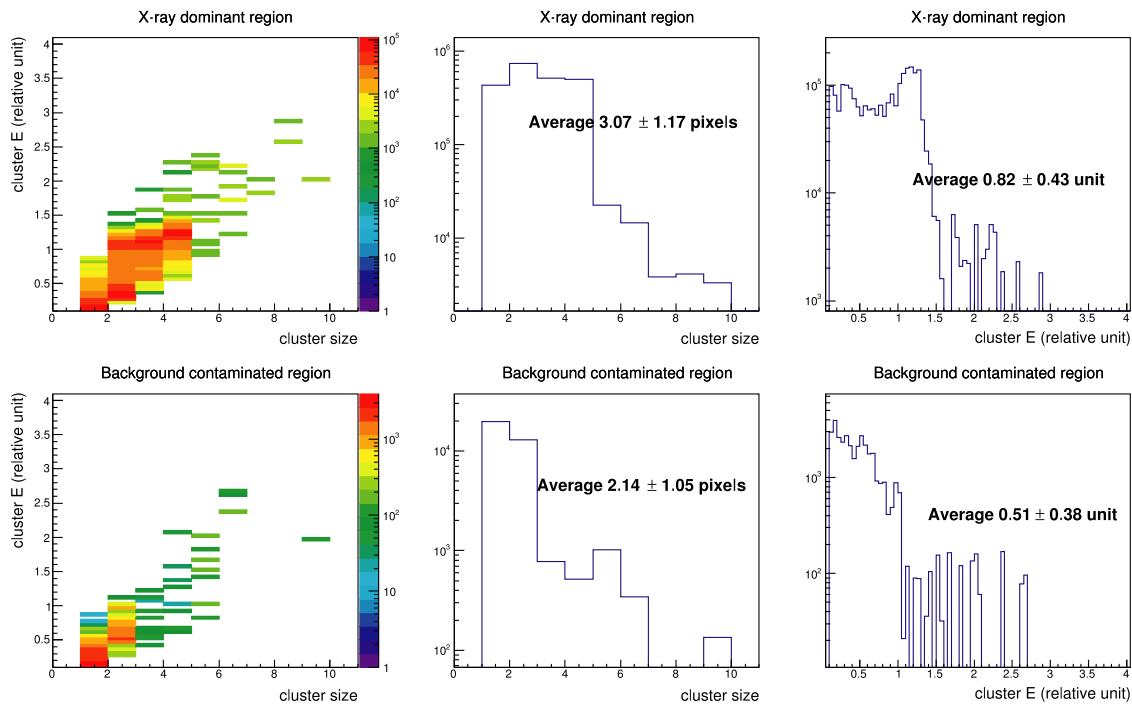


Fig. 3. With the 24.99 keV X-rays, cluster energy versus cluster size (left), cluster size (middle) and cluster energy (right) of the Pixelink sensor in the source dominant region (top) and background contamination region (bottom) measured by the Pixelink silicon sensor.

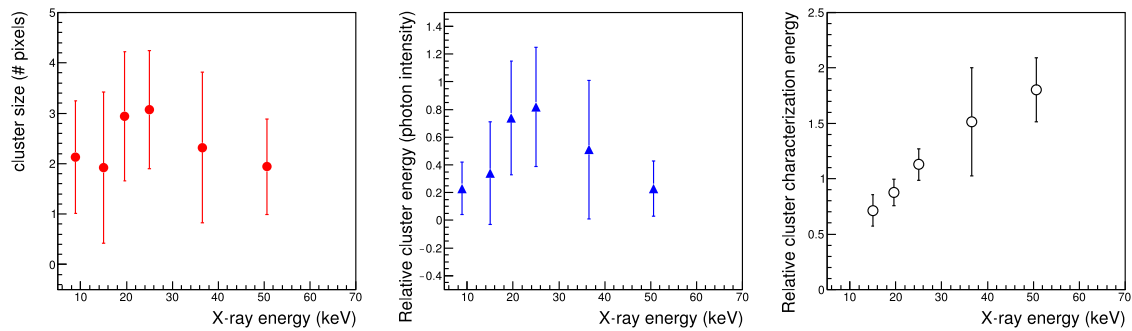
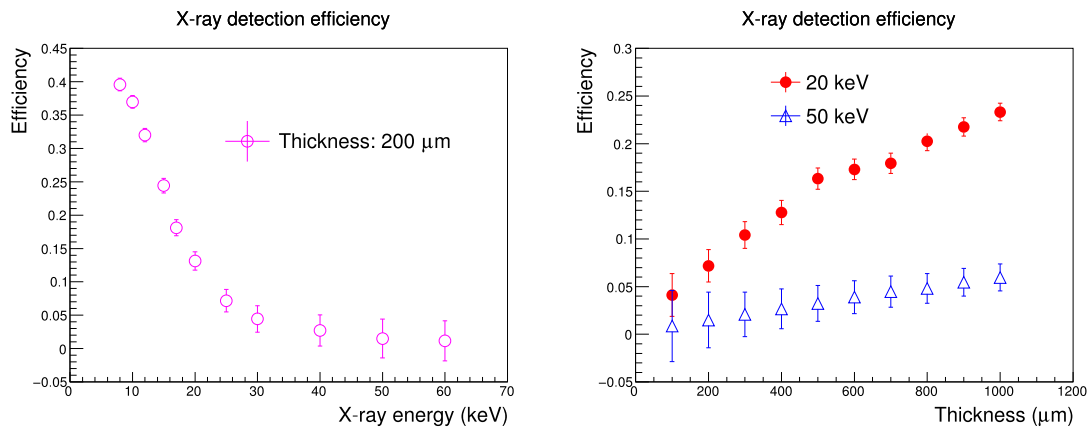


Fig. 4. X-ray energy dependence of average cluster size (left), average cluster energy (middle) and the cluster characterization energy (right) measured by the Pixelink silicon sensor.



(a) X-ray energy dependent detection efficiency for 200 μm thick silicon sensor.

(b) Silicon sensor thickness dependent X-ray detection efficiency

Fig. 5. Energy and silicon sensor thickness dependent X-ray detection efficiency in a simulation using the FLUKA 2011.2x.3 package. The energy dependence is shown in (a) and the silicon sensor thickness dependence is shown in (b).

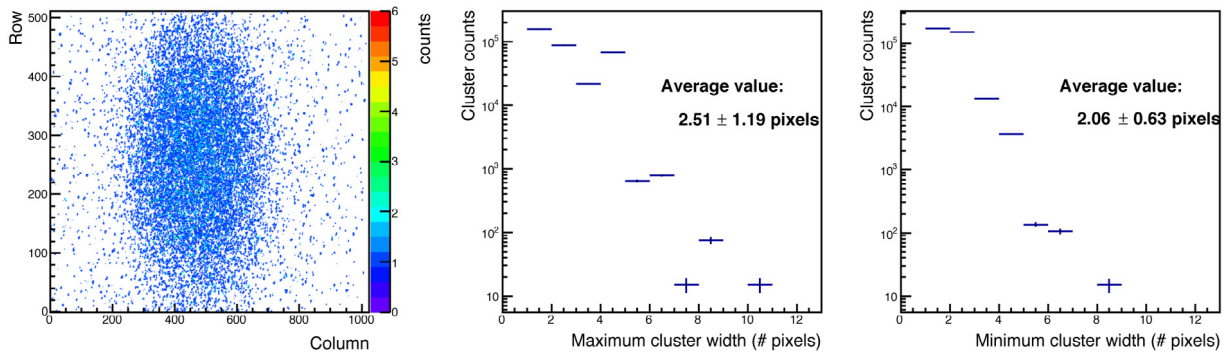


Fig. 6. 24.99 keV X-ray source test with the ALICE MAPS. The 2D imaging of the X-ray source by the MAPS sensor is shown in the left panel, the distribution of the maximum cluster width is shown in the middle panel and the distribution of the minimum cluster width is shown in the right panel.

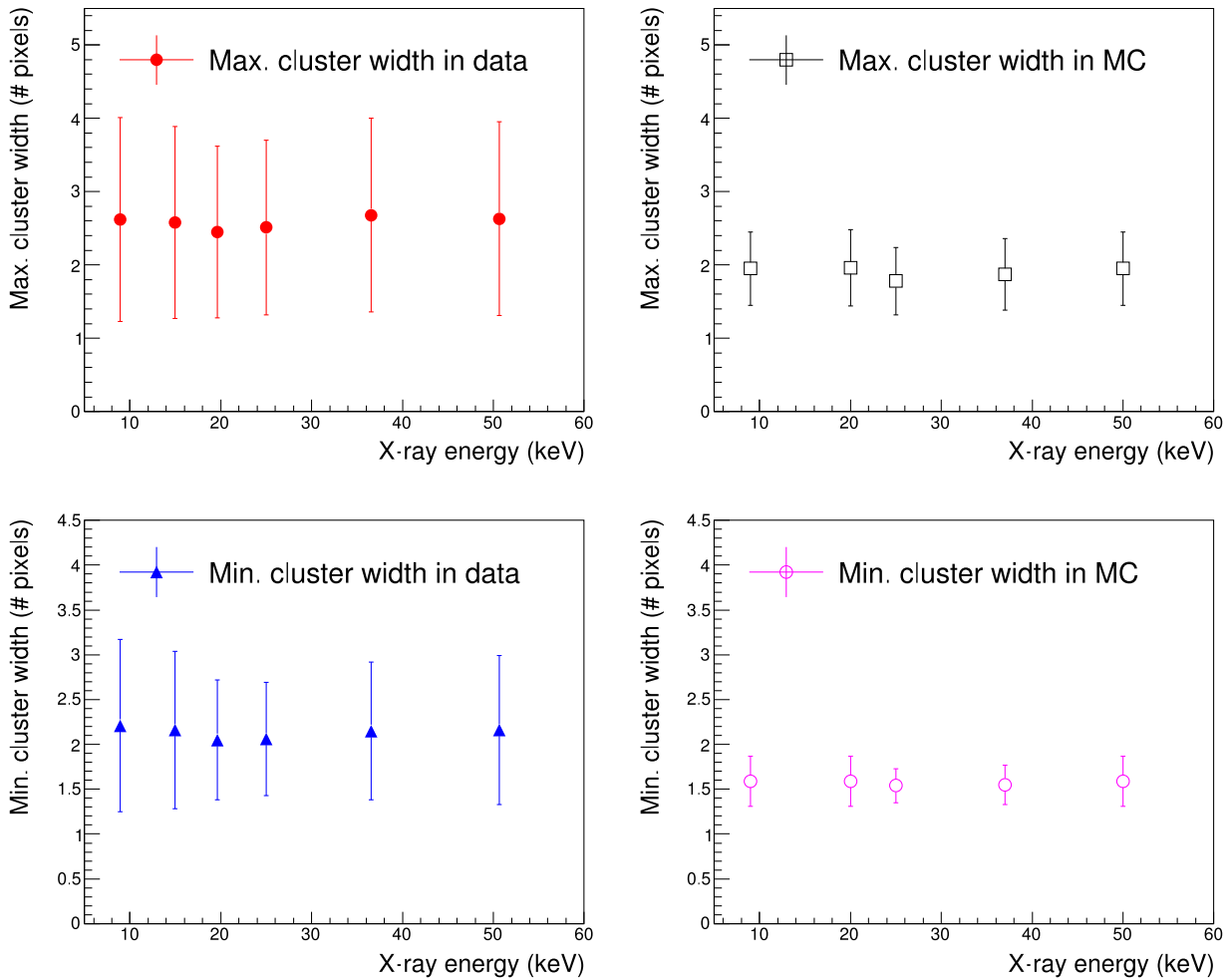


Fig. 7. Top panel shows the X-ray energy dependence of average maximum cluster width in data (left) and simulation (right). Bottom panel shows the X-ray energy dependence of average minimum cluster width in data (left) and simulation (right).

2011.2x.3 package [3] is used to simulate the single layer Pixelink X-ray source test as configured for the real data. Fig. 5a shows the X-ray energy dependent detection efficiency for 200  $\mu\text{m}$  thick silicon sensor and Fig. 5b shows the silicon sensor thickness dependent detection efficiency for simulated 20 keV and 50 keV X-rays. The X-ray detection efficiency decreases as X-ray energy increases (see Fig. 5a) and it increases as the silicon sensor thickness increases (see Fig. 5b). Taking the 200  $\mu\text{m}$  silicon sensor for example, even the detection efficiency for 20 to 50 keV X-rays is between 1% to 9%, it is still capable to perform ultrafast X-ray imaging using silicon detectors with high flux X-ray beam facility.

The same X-ray test setup as shown in Fig. 2a was used to study the MAPS sensor performance. As digitization is processed on MAPS sensor, only pixel address and one bit hit information is stored in the offline data. The MAPS pixel clusters were searched using the same cluster finder algorithm as in the Pixelink sensor test. To better characterize the cluster shape, the maximum cluster width and the minimum cluster width were used. Fig. 6 shows the direct measurements of the MAPS sensor with 24.99 keV X-rays. A clear image of the X-ray source has been obtained. The distributions of maximum (minimum) cluster width from the 24.99 keV X-ray test are shown in the middle (right) panel of Fig. 6.

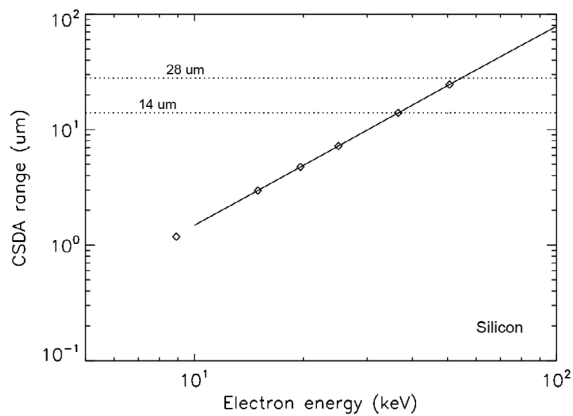


Fig. 8. The X-ray energy dependent CSDA range for silicon. Open points highlight the X-ray source energy values for the tests discussed in this paper.

The energy of the  $^{241}\text{Am}$  source was scanned and the average maximum and minimum cluster width have been extracted for each X-ray energy. The X-ray energy dependent average maximum (minimum) cluster width measured in data are summarized as the solid points shown in the left panels of Fig. 7. The cluster shape has also been studied with the FLUKA 2011.2x.3 simulation with the X-ray source test configuration, and the simulation results are listed as the open points shown in the right panels of Fig. 7. Even though the simulation of detector response effects (such as the charge sharing between adjacent pixels) is under development, no significant energy dependence is seen in either data and simulation. The measured MAPS sensor cluster size from the preliminary X-ray tests is larger than the CSDA model [4] prediction as shown in Fig. 8. The difference might be due to charge diffusion and collection process, the sensor geometry and other effects

which cannot be described by the CSDA model. The feasibility test results suggest that ultrafast silicon sensor with wider dynamic range are required to store the photon or electron energy information for the X-ray imaging.

### 3. Summary and outlook

Initial test results of the Pixelink silicon sensor and the ALICE MAPS sensor using an X-ray source producing 8.91 keV to 50.65 keV X-rays provide the first proof-of-principle evidence and guidance for hard X-ray silicon imaging capability. Preliminary simulation results also prove the feasibility of using silicon detectors for hard X-ray imaging. Ongoing R&D work of new ultrafast thin silicon sensor techniques such as the High Voltage Monolithic Active Pixel Sensor will provide new options for hard X-ray imaging in the laboratory using sealed sources and in future beam tests at APS.

### Acknowledgments

This work was funded by the U.S. Department of Energy (DOE)-Office of Science, Nuclear Physics and the Los Alamos National Laboratory C2 program.

### References

- [1] B. Abelev, et al., Technical Design Report for the Upgrade of the ALICE Inner Tracking System, 2013 CERN-LHCC-2013-024, ALICE-TDR-017.
- [2] M. Krammer, et al., Study and Development of a novel Silicon Pixel Detector for the Upgrade of the ALICE Inner Tracking System, 2015 CERN-THESIS-2015-255.
- [3] T.T. Bhlen, F. Cerutti, M.P.W. Chin, A. Fass, A. Ferrari, P.G. Ortega, A. Mairani, P.R. Sala, G. Smirnov, V. Vlachoudis, The FLUKA code: Developments and challenges for high energy and medical applications, Nucl. Data Sheets 120 (2014) 211–214.
- [4] H. Bichsel, Stragglings in thin silicon detectors, Rev. Modern Phys. 60 (3) (1988) 663–669.